Asymmetric Catalysis

How to cite:
International Edition: doi.org/10.1002/anie.202106142
German Edition: doi.org/10.1002/ange.202106142

Indolizy Carbene Ligand. Evaluation of Electronic Properties and Applications in Asymmetric Gold(I) Catalysis

Thibaut Martinez, Avassaya Vanitcha, Claire Troufflard, Nicolas Vanthuyne, Jérémy Forté, Geoffrey Gontard, Gilles Lemière, Virginie Mouriès-Mansuy,* and Louis Fensterbank**

Dedicated to Prof. Christian Bruneau for his outstanding contribution to catalysis

Abstract: *We report herein a new family of carbene ligands based on an indolizine-ylidene (Indolizy) moiety. The corresponding gold(I) complexes are easily obtained from the gold(I)-promoted cyclization of allenylpyridine precursors. Evaluation of the electronic properties by experimental methods and also by DFT calculations confirms strong σ-donating and π-accepting properties of these ligands. Cationization of the gold(I) complexes generates catalytic species that trigger diverse reactions of (poly)unsaturated precursors. When armed with a methylene phosphine oxide moiety on the stereogenic center adjacent to the nitrogen atom, the corresponding bifunctional carbene ligands give rise to highly enantioselective heterocyclizations. DFT calculations brought some rationalization and highlighted the critical roles played by the phosphine oxide group and the tosylate anion in the asymmetric cyclization of γ-allenols.*

Introduction

The last decades have witnessed a strong expansion in homogeneous gold catalysis promoting a broad range of organic transformations.[1] The high π-Lewis acidity of cationic gold(I) complexes allow them to activate various unsaturations such as alkynes, allenes and also alkenes towards intra- or intermolecular nucleophilic addition.[2] During the process, the ligands carried by the gold(I) center play a major role in terms of stability, allowing low catalyst loadings, modulation of activity, and selectivity.[3] Furthermore, the linear coordination of gold(I) complexes that positions the ancillary ligand opposite to the substrate and thus to the outer-sphere attack of the nucleophile renders asymmetric gold catalysis a challenging goal.[4] The role of the chiral ligand is therefore crucial notably by constraining the degrees of freedom of the system. In this context, *C*-ligands such as *N*-heterocyclic carbenes (NHCs **A**)[5] have exhibited high potential. More accessible than a lot of phosphine ligands that are tedious to prepare and prone to oxidation, they have the ability to form stable complexes thanks to strong σ-bonding with the gold metallic center while π-backbonding to the carbene will be highly dependent from its structural features, the interplay of both effects leading to specific reactivities.[6] In 2005, the group of Bertrand[7] developed a new class of carbenes, the cyclic (alkyl)-(amino)carbenes (CAACs **B**) in which a nitrogen of a classical NHC diaminocarbene was replaced by a carbon atom. Those are more σ-donating and π-accepting than the parent NHCs.[8] The corresponding gold complexes[9] have led to the first examples of hydroamination of alkynes and allenes using ammonia or hydrazine.[10] The replacement of the alkyl substituent of CAACs by an aryl leads to the formation of new cyclic (amino)(aryl)carbenes (CAArCs **C**),[11] that still feature high nucleophilicity but also enhanced electrophilicity resulting in a smaller single-triplet gap than for CAACs.

The implementation of asymmetric gold-catalyzed processes relying on monodentate *C*-ligands has initially consisted in the introduction of stereogenic centers on the imidazolium backbone or on the *N*-ligated substituents.[12,13] Tomioka and coll.[14] synthesized the first chiral C_2-symmetric dihydroimidazol-2-ylidene gold(I) complexes and applied them in a moderately enantioselective methoxycyclization of 1,6-enynes (up to 59% *ee*). Improved enantioselectivities (above 70%) for similar reactions were observed using C_2-symmetric NHC complexes bearing bulky stereogenic *N*-substituents.[15,16] Still, these systems suffer from the fact that the nitrogen substituents are too remote from the gold center to fix an adequate steric environment and several strategies for the introduction of higher performance elements of chiral discrimination have been proposed to render carbenes the ligands of choice for asymmetric gold-catalyzed transformations.[17,18] Notably, NHC-type ligands based on an imidazo-[1,5-a]pyridine-3-ylidene (ImPy **D**) skeleton, initially disclosed by the groups of Lassaletta and Glorius have allowed the synthesis of new families of carbene ligands by the introduction of substituents at the C5 position. The latter are in close proximity to the metal-center and can be designed to convey properties to the gold complexes.[21] For instance, the π-acceptor properties of ImPy ligands were enhanced by the introduction of a cyclophane scaffold and found applications in the catalysis of the cycloisomerization of ene-allenes.[19] The substitution at the C5 position constitutes also an opportunity to provide axially chiral complexes.[22] Zhang

[*] Dr. T. Martinez, Dr. A. Vanitcha, C. Troufflard, J. Forté, G. Gontard, Dr. G. Lemière, Dr. V. Mouriès-Mansuy, Prof. L. Fensterbank
Institut Parisien de Chimie Moléculaire, Sorbonne Université, CNRS
4 Place Jussieu, CC 229, 75252 Paris Cedex 05 (France)
E-mail: gilles.lemiere@sorbonne-universite.fr
virginie-mansuy@sorbonne-universite.fr
louis.fensterbank@sorbonne-universite.fr
Dr. N. Vanthuyne
Aix Marseille Univ, CNRS, Centrale Marseille, iSm2
13397 Marseille Cedex 20 (France)
Supporting information and the ORCID identification number(s) for the author(s) of this article can be found under: https://doi.org/10.1002/anie.202106142.

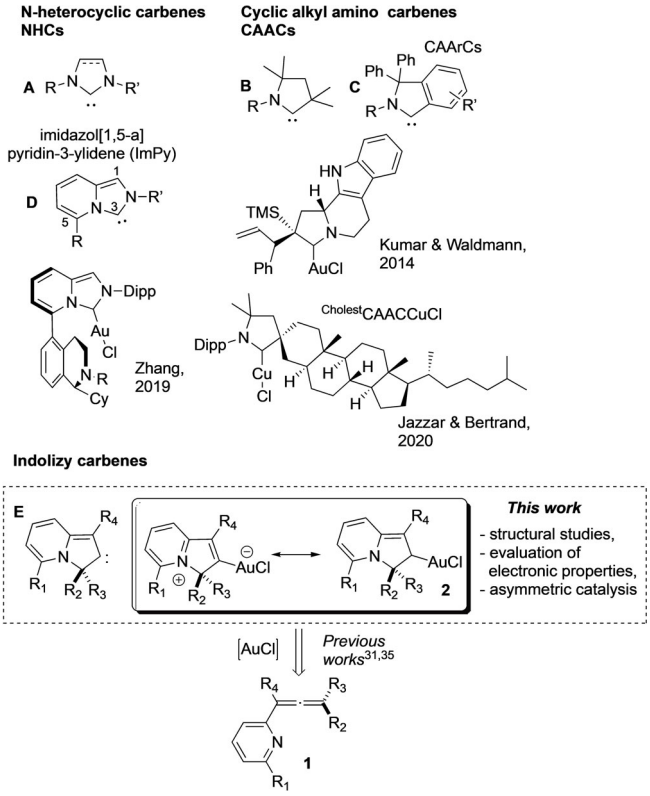

Figure 1. Milestones in the development of Au^{I}-carbene complexes and presentation of the work.

further refined this approach by providing chiral bifunctional NHC ligands flanked with a tetrahydroisoquinoline moiety at the C5 position.[23] The corresponding gold complexes proved to be competent in a series of asymmetric transformations (Figure 1).

Regarding CAACs, the presence of a quaternary carbon center adjacent to the ylidene carbon is a good lever to introduce stereogenicity close to the active site. Bertrand and coll. initially prepared an enantiopure (−)-menthol derived CAAC ligand[7a] but no asymmetric catalysis in a copper-catalyzed asymmetric conjugated borylation reaction was recorded,[24] this being certainly due to a conformational inversion of the menthyl group. In contrast, a more rigid CAAC with extended chirality derived from a 5α-cholestan-3-one steroid backbone was recently synthesized and the corresponding copper complex ^{Cholest}CAACCuCl, promoted encouraging enantioselectivity (55 % *ee*) in the same borylation reaction.[24,25] It should also be noted that racemic chiral CAACAuCl complexes have been prepared by Kumar and Waldmann via a Me_2SAuCl-promoted cyclization-rearrangement sequence of 1,7-enynes and two examples of catalysis were given.[26]

As part of our ongoing interest in the design of new chiral ligands for gold complexes[27–29] we have devised the new family of Indolizy *C*-ligands **E**, possibly bifunctional[30] (Figure 1). While direct isolation of these ligands has not been accomplished so far, we found more convenient to directly access to the corresponding gold complexes **2** through an efficient gold-promoted cyclization of allenepyridines of type **1** that we previously worked out.[31,32] Two resonance forms can be written for complexes of type **2**, vinylgold vs. carbene, but the very short Au−C bond distance (1.993(4) Å) on **2a**,[33] reminiscent of other gold carbenes,[34] suggested a carbenic character favorable for catalytic applications. Overall, the ligands **E** connected to the gold center of complexes **2** could be considered as the first examples of vinylogous CAACs[7] that also include chiral congeners.

Prompted by a recent report from the Muñoz group on a related use of bis-pyridyl allenes **1** (R_1 = Me, R_2 = 2-methylpyridine) as precursors of gold carbenes and their preliminary catalytic activity,[35] we herein extend the family of gold(I) complexes **2**, evaluate the electronic properties conferred by ligands **E** and study their catalytic applications notably in enantioselective gold(I) catalysis.

Results and Discussion

Preparation of a Family of Gold(I) Complexes 2

We synthesized a wide range of gold(I) complexes **2** including achiral complex **2b** and chiral complexes **2a** and **2c**–**k**. As depicted in Scheme 1, they were obtained in two steps from propargyl acetates **3** and **3′**. S_N2' reactions on the latter provided various pyridyl-allenes **1** that were engaged in the previously mentioned cyclization reaction using 1 equiv of Me_2SAuCl to smoothly deliver complexes **2**.[31] Through this route, we could control strategic positions on chiral complexes (±)-**2**: i) the nature of the stereogenic center, either devoid of an additional coordinating group (**2c**) or flanked with a β-phosphorus group (phosphine oxide for **2a** and **2d**–**g** featuring an increasing steric demand, phosphine sulfide for **2h** and phosphonate for **2i**), ii) the vinyl position close to the gold(I) center by varying the aryl scaffold through the introduction of a 4,6-dimethylphenyl moiety (complexes **2d** and **2f**). The obtained cyclization yields for complexes **2**, from quantitative for **2a**–**c** to 34 % for **2f** were relatively consistent with the steric bulk imposed by the substituents of the allene moieties and gave sufficient material for catalytic trials. X-ray diffraction (XRD) analyses were obtained for complexes **2c**–**2f**.[33] The Au−C bond lengths lie in the same range from 1.990(6) Å for **2d** to 2.002(1) Å for **2f**. As shown also on Scheme 1, for complexes **2** bearing a phosphine oxide, a stabilising dipole-dipole interaction between the oxygen of the phosphine oxide and the nitrogen atom of the *N*-containing 6-membered ring seems to operate with an average O-N distance of 2.95 Å.

To obtain enantiomerically pure complexes **2**, we relied on a total chirality transfer in the gold-promoted cyclization.[31] This could be accomplished from allene (−)-**1a** to give precatalyst catalyst (−)-(*S*)-**2a** whose absolute configuration was determined by XRD.[36] Nevertheless, we found more convenient to obtain each enantiomer of complexes **2a** and **2c**–**i** by preparative chiral HPLC.[37] It should be noted that thiophosphine complex **2h** could not be resolved and proved unstable in the HPLC conditions. We were also able to directly obtain enantiopure indolizy-gold(I) complexes **2j** and **2k** using inexpensive (−)-menthone from the chiral pool.[7] In

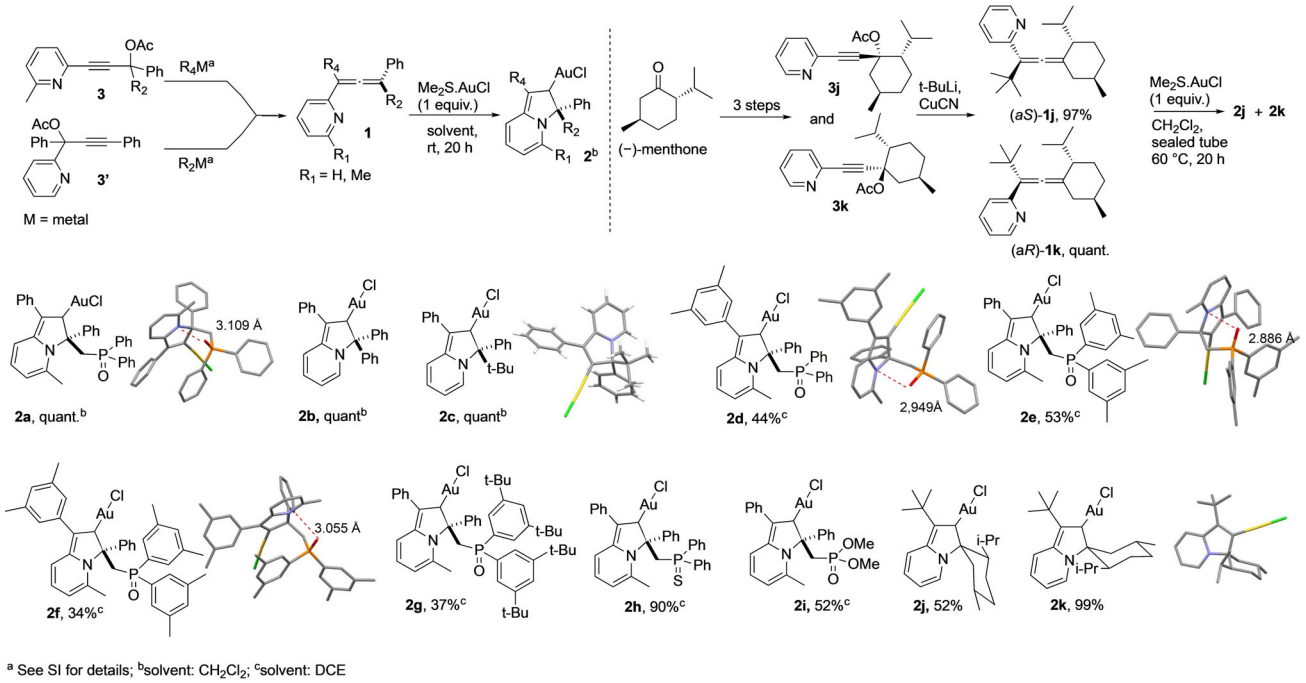

[a] See SI for details; [b]solvent: CH_2Cl_2; [c]solvent: DCE

Scheme 1. Indolizy Au^I precatalysts **2**.

three steps including initially the addition of ethynylmagnesium bromide onto (−)-menthone,[38] a mixture of two separable diastereoisomeric propargylic acetates **3j** and **3k** was obtained. Subsequent cuprate addition led to the formation of tetrasubstituted allenes as single diastereomers in an excellent yield of 97% for both (*aS*)-**1j** and (*aR*)-**1k**. Finally, the corresponding chiral gold(I) complexes **2j** and **2k** were obtained in, respectively 52% and 99% yield, by stereospecific reaction with Me_2SAuCl. The structure of **2k** was confirmed by XRD analysis (see SI).[39]

Evaluation of the Electronic Properties

The modification of the NHC backbones can dramatically change their electronic features.[40] Based on this fact, we have first determined the geometries and energies of the frontier orbitals for the free ligand **Indolizy-b** of complex **2b** (see also Figure 2) by means of DFT calculations at the B3LYP/def2-TZVP level of theory. It was found that the HOMO of **Indolizy-b** (−4.97 eV) lies considerably higher than those calculated for relevant CAACs considered as very good σ-donor ligands. This data highlights the tendency of the ylidene carbon to increase its electron-donating ability when decreasing the number of electronegative nitrogen atoms connected to it.[41]

Intriguingly, **Indolizy-b** exhibits a LUMO lying at a very low energy level that is at first glance suggestive of an exceptional π-acidity for this ligand, comparable to the coumaraz-2-one-4-ylidene carbene.[42] Nevertheless, π-acceptor capabilities correlate with the energies of the relevant π*-orbitals and not necessarily the LUMO so that the sole consideration of the LUMO energy can be misleading.[43] Visualization of the shape of the frontier orbitals allows for a qualitative estimation of their geometrical appropriateness for a possible overlap with the metals d-orbitals. While the HOMO of **Indolizy-b** is mainly located on the ylidene carbon, the LUMO is rather opposite to this site and mainly delocalized over the *N*-containing 6-membered ring (Figure 2b). Interestingly, the LUMO + 1 that lies slightly higher than the one

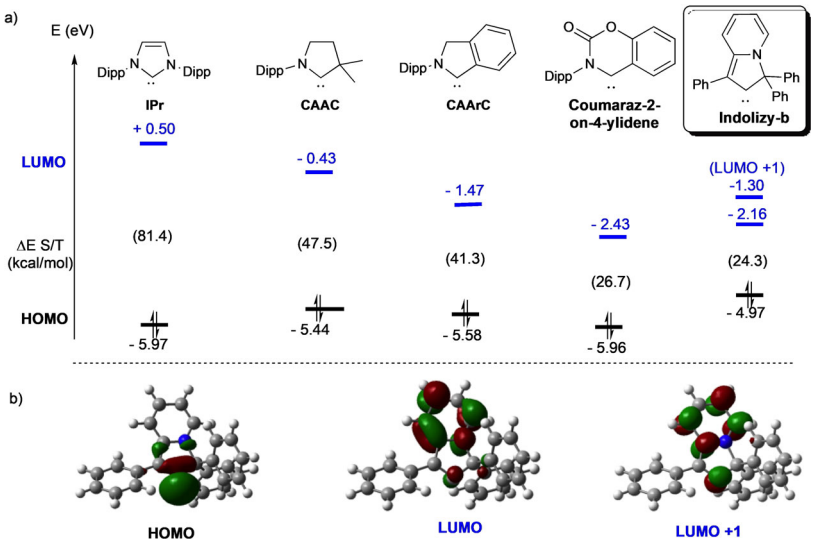

Figure 2. a) Relevant HOMOs and LUMOs (present on the ylidene carbon) energy levels and singlet-triplet transition energy of a series of relevant NHC including **Indolizy-b** calculated at the B3LYP/def2-TZVP level of theory b) Vizualisation of the frontier orbitals of **Indolizy-b** plotted with Gaussview at an isosurface value of 0.05 au.

calculated for a highly π-acidic CAArC[11] (−1.30 vs. −1.47), is much present on the ylidene carbon and therefore can also account for the overall π-acidity of the ligand. Finally, **Indolizy-b** presents a very small singlet-triplet gap (24.3 kcal mol^{-1}) smaller than the one calculated for the coumaraz-2-one-4-ylidene carbene (26.7 kcal mol^{-1}), which presages good bonding abilities.[44]

To experimentally corroborate these calculations, we first gauged the donating ability of the Indolizy ligand following the Huynh Electronic Parameter (HEP). This method, initially based on the ^{13}C NMR spectroscopy analysis of trans-[$PdBr_2$(*i*Pr_2-bimy)L] (*i*Pr_2-bimy = 1,3-diisopropylbenzimidazolin-2-ylidene) complexes on which L is a NHC ligand, has also been transposed to [Au(*i*Pr_2-bimy)L] gold(I) complexes.[45,46] While the HEP method has never been used for the evaluation of the σ-donation of CAACs or analogues, we nevertheless synthesized the [Au(*i*Pr_2-bimy)(**Indolizy-b**)]BF_4 complex **5** in good yield (84%) through a one-pot reaction by mixing *i*Pr_2-bimyH$^+BF_4^-$ (**4**) in the presence of K_2CO_3 and gold complex **2b** (Scheme 2). The structure of **5** was secured

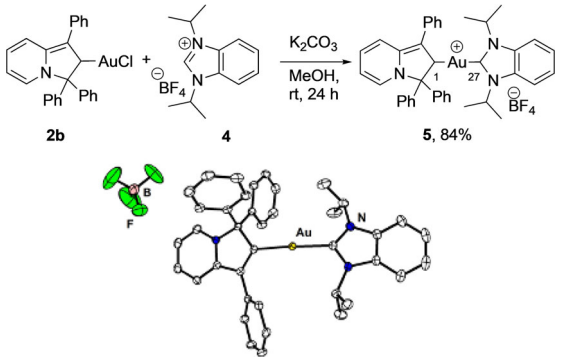

Scheme 2. Synthesis of complex **5** and its XRD structure (hydrogen atoms are omitted for clarity). Selected bond lengths [Å] and angle [deg]: Au1–C27 2.035(3), Au1–C1 2.033(3), C1-Au1-C27 174.5(1)°.

by XRD analysis.[47] As expected, a linear coordination pattern in which the central gold(I) atom is both coordinated to the *i*Pr_2-bimy and **Indolizy-b** ligands was observed. The isopropyl C–H protons of complex **5** appeared by ^1H NMR as a multiplet at 5.05 ppm, falling in the range of the expected values for this type of complexes, and which indicated a free rotation around the Au-$C_{carbene}$ bonds.[45] Moreover, the ^{13}C NMR spectrum of **5** exhibited two carbene resonances at 193.1 ppm, presumably for the *i*Pr_2-bimy carbene and more downfield at 204.5 ppm for the Indolizy ligand. A two dimensional HMBC NMR analysis confirmed these assignments (see SI). Based on the linear correlation between the $^{13}C_{carbene}$ (*i*Pr_2-bimy) values for the Pd^{II} and Au^{I} complexes, a HEP value of 184.7 ppm, corresponding to the highest HEP value ever found for a carbene ligand, and much higher than the HEP of IPr (177.5 ppm), was determined for the Indolizy ligand. It therefore appears that Indolizy ligand features strong σ-donating properties which fits with the DFT calculations.

Next, the π-acceptor character of the Indolizy ligand was assessed by measuring the ^{77}Se NMR chemical shift of the

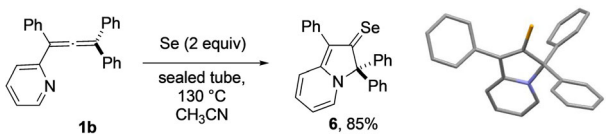

Scheme 3. Synthesis of Indolizy selenide derivative **6**.

selenium derivative **6**,[48,49] prepared in 85% yield by mixing in acetonitrile elemental selenium with allene **1b** at 130 °C in a sealed tube for 22 h (Scheme 3).[50] The structure was ascertained by a single crystal XRD analysis.[51]

With a δ ^{77}Se NMR value of 566.7 ppm in [D_6]acetone and 528.1 ppm in $CDCl_3$, Indolizy ligand appears far more π-accepting than IPr (δ ^{77}Se: 87.0 ppm in [D_6]acetone)[48] but slightly less π-accepting than the CAArC of Figure 2 (δ ^{77}Se: 601 ppm).[11] Interestingly this last finding is also consistent with the above-presented DFT study.

We also examined the impact of the electronic properties of the Indolizy ligand by using the gold(I) precatalyst **2a** in a diagnostic reaction consisting in the cycloisomerization of allene-diene **7** (Scheme 4). It was shown that in this trans-

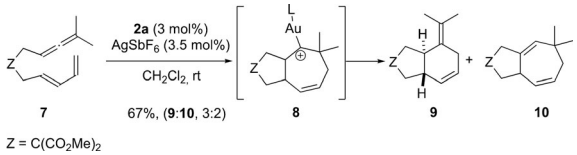

Scheme 4. Diagnostic reaction using the allenediene precursor **7**.

formation the π-activation of the allene by a cationic gold(I) catalyst triggers the generation of a cationic intermediate **8**. The latter can evolve following two pathways depending on the influence of the ancillary ligand: an alkyl shift or a 1,2-hydride shift giving, respectively the [4+2] cycloadduct **9** or the [4+3] cycloadduct **10**.[52] Bicyclic product **10** is a marker of a strong donor ligand which favors a carbene reactivity of intermediate **8**. For instance IPr or IMes ligand will provide almost exclusively **10**.[52] In contrast, hydrindane product **9** suggests a cationic pathway because of the reduced donation of the ancillary ligand. This is what happens when using π-accepting cyclophane-NHCs which yields a 72:28 ratio of **9** vs. **10**.[21] In the presence of $AgSbF_6$ and **2a**, a 74:26 mixture of cycloadducts **9** and **10** was obtained in 67% yield. While this type of ratio has to be taken cautiously since steric effects can also be at play,[52e] the convergence between the ^{77}Se NMR value and this experiment suggests significant π-acidic properties of the Indolizy ligand.

Applications in Asymmetric Catalysis

Besides the cyloisomerization of **7**, we checked the reactivity of precatalyst **2a** in a few diagnostic reactions (see SI). Consistent results with literature were obtained. We also checked the configurational stability of (−)-(*S*)-**2d** in thermal conditions (80 °C for 24 h, see SI). All these positive data

Table 1: Methoxycyclization reaction.

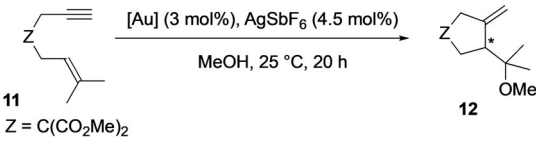

Entry	[Au]	Yield of **12** [%]	e.r.[a] (*R*:*S*)[b]
1	(−)-(*S*)-**2a**	92[c]	59:41
2	(+)-**2c**	97[c]	50:50
3	(−)-(*S*)-**2d**	76	54:46
4	(−)-(*R*)-**2e**	76	38:62
5	(+)-(*S*)-**2f**	95	64:36

[a] Enantiomeric ratios were determined by chiral HPLC; [b] The configurations were assigned by comparison with literature [29]; [c] NMR yields with trimethoxybenzene as internal standard.

drove us to test asymmetric catalysis with Indolizy-Au complexes **2** (except **2h**)[53] We first studied the methoxycyclization of enyne **11** that has served as benchmark reaction in numerous studies.[29] Using typical conditions ($AgSbF_6$ as cationizing agent in MeOH at rt), low enantioselectivities were recorded, the best result of 28% *ee* being obtained with complex (+)-(*S*)-**2f** (Table 1, entry 5). Interestingly, a precatalyst bearing a gem-dialkyl group ((+)-**2c**) with no additional functionality provided a racemic mixture (entry 2) while the other complexes bearing a phosphine oxide substituted arm allowed some tangible enantiomeric discrimination.

Based on these promising findings, we examined the purely intramolecular gold-catalyzed hydroalkoxylation of 4,5-hexadien-1-ols **13a** and **13b** and the results are summarized in Table 2. Precatalysts **2** were first activated with a silver salt before the addition of substrates **13**. We started our studies with gold(I) complex (−)-(*S*)-**2a** and initially checked the influence of the silver salt as cationizing agent on the enantioselectivity of the reaction. At 25 °C with $AgSbF_6$ in toluene (entry 1), low yield of **14a** (16%) was obtained with almost no enantioselectivity (e.r. = 45:55). Increasing the temperature to 50 °C (entry 2) resulted in a yield increase (52%) but a decrease of enantioselectivity. Keeping this temperature with other silver salts (entries 3,4), low yields of **14a** in racemic form were observed.

Interestingly, with AgOTs at 25 °C,[54] tetrahydrofuran **14a** was obtained quantitatively with a promising enantiomeric ratio of 70:30 (entry 5). The absolute configuration of the (*S*)-major enantiomer was assigned by comparison with previous chiral HPLC data and optical rotation.[55] From a second set of experiments with AgOTs, we showed that the reaction does not work at temperatures below 10 °C and that no enantioselectivity was observed (entries 6–8). From all these experiments, we converged to catalytic reactions at 25 °C with AgOTs as chloride scavenger as in entry 5. Screening of the gold complexes brought intriguing findings. We confirmed that for complexes **2k**, **2j** and **2c** that do not bear a phosphine oxide moiety, the yields were excellent but quasi-racemic mixtures were obtained (entries 9–11). In contrast, for complex (+)-(*R*)-**2d** bearing a phosphine oxide moiety, enantioselectivity was restored (e.r. = 27:73, entry 12). This slight improvement compared to (−)-(*S*)-**2a** could be ascribed to the larger steric hindrance in vicinity of the gold(I) center brought by the 3,5-dimethylphenyl group on the vinyl carbon. The introduction of 3,5-dimethylphenyl groups on the phosphorus atom as for (−)-(*R*)-**2e** significantly increased the enantiomeric ratio to 12:88 (entry 13). As previously shown, the decrease or increase in temperature did not improve the enantioselectivities (entries 14 and 15). Gratifyingly, combining both previous steric constrains by using (−)-(*R*)-**2f** yielded the best e.r. value of 8:92 (entry 16). This also corresponds to the best e.r. obtained on **14a** with a carbene gold complex.[17,56] Using gold(I) complex (*R*)-**2g** bearing two 3,5-di-tert-butylphenyl groups on the phosphorus atom led however to a lower enantioselectivity (entry 17), suggesting that the steric hindrance around the phosphorus atom does not seem to be the sole factor to influence the enantioinduction. Finally, substitution of the phosphine oxide moiety by a phosphonate ((−)-**2i**) moiety proved to be highly detrimental to the enantioselectivity (entry 18) giving a e.r. of 57:43. Allenol **13b** gave similar

Table 2: Intramolecular hydroalkoxylation.

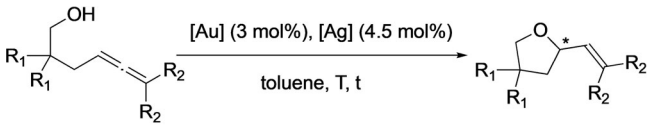

13a, R_1 = Ph, R_2 = H
13b, R_1 = H, R_2 = -C_5H_{10}-

14a, R_1 = Ph, R_2 = H
14b, R_1 = H, R_2 = -C_5H_{10}-

Entry	[Au]	[Ag]	*T* [°C]	*t* [h]	Yield of **14a** [%]	e.r.[a] (*S*:*R*)[b]
1	(−)-(*S*)-**2a**	$AgSbF_6$	25	30	16	45:55
2	(+)-(*R*)-**2a**	$AgSbF_6$	50	*16*	52	49:51
3	(−)-(*S*)-**2a**	AgOTf	50	16	28	51:49
4	(+)-(*R*)-**2a**	$AgNTf_2$	50	26	28	50:50
5	(−)-(*S*)-**2a**	AgOTs	25	5	quant.	70:30
6	(−)-(*S*)-**2a**	AgOTs	−20	19	–	–
7	(−)-(*S*)-**2a**	AgOTs	0	5	–	–
8	(+)-(*R*)-**2a**	AgOTs	10	7	34	41:59
9	**2j**	AgOTs	25	2	quant.	50:50
10	**2k**	AgOTs	25	2	quant.	51:49
11	(+)-**2c**	AgOTs	25	2	quant.	52:48
12	(+)-(*R*)-**2d**	AgOTs	25	3.5	quant.	27:73
13	(−)-(*R*)-**2e**	AgOTs	25	2.5	quant.	12:88
14	(−)-(*R*)-**2e**	AgOTs	−20	5 d	quant.	24:76
15	(−)-(*R*)-**2e**	AgOTs	50	1.5	quant.	13:87
16	(−)-(*R*)-**2f**	AgOTs	25	1.5	quant.	8:92
17	(*R*)-**2g**	AgOTs	25	1.5	quant.	27:73
18	(−)-**2i**	AgOTs	25	22	quant.	57:43
Entry	[Au]	[Ag]	*T* [°C]	*t* [h]	Yield of **14b** [%]	e.r.[a]
19[c]	(−)-(*S*)-**2a**	$AgSbF_6$	25	16	81%	49:51
20	(+)-(*R*)-**2a**	AgOTs	25	16	quant.	60:40
21	(+)-(*R*)-**2d**	AgOTs	25	1.5	quant.	58:42
22	(−)-(*R*)-**2e**	AgOTs	25	1.5	quant.	74:26
23	(+)-(*S*)-**2f**	AgOTs	25	1.5	quant.	23:77

[a] Enantiomeric ratios were determined by chiral HPLC. [b] The configurations were assigned by comparison with literature [55]. [c] The reaction was run in DCM.

Table 3: Intramolecular hydroamination.

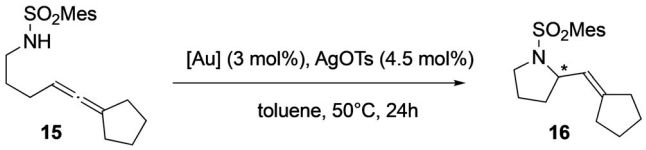

Entry	[Au]	Yield of **16** [%]	e.r.[a]
1	(+)-(*R*)-**2a**	71	28:72
2	(+)-(*R*)-**2d**	74	25:75
3	(−)-(*R*)-**2e**	66	15:85
4	(−)-(*R*)-**2f**	66	17:83
5	(*S*)-**2g**	66	70:30
6	(−)-**2i**	48	55:45

[a] Enantiomeric ratios were determined by chiral HPLC.

results with each catalyst **2**, the highest enantioselectivity being recorded with (+)-(*S*)-**2f** (entry 23).

The asymmetric intramolecular hydroamination of sulfonamide **15** was next examined. As shown in Table 3, pyrrolidine derivative **16** was obtained in moderate to good yields in 24 h hours at 50 °C (Table 2, entries 1–6). The enantiomeric ratios followed the same trend as described for γ-allenols **13** with the same catalysts. As for **13b**, the use of precatalysts (−)-(*R*)-**2e** and (−)-(*R*)-**2f** did not make real difference in terms of enantioselectivity (entries 3 and 4).

Mechanistic Aspects

As discussed above, analysis of the XRD structures of most of the neutral chlorinated gold complexes **2** revealed that the privileged conformation is the one where the phosphine oxide moiety is directly pointing towards the *N*-containing heterocyclic ring (Scheme 1). However, the gold catalysts are effective under their cationic form after abstraction of the chloride ligand. We attempted to crystallize the cationic form of the gold complex (±)-**2a** (as a racemic mixture) after anion metathesis using a stoichiometric amount of silver triflimidate.[57] The expected cationic complex (±)-**17** was formed and its XRD structure[58] revealed a dimeric complex with a Au-Au distance of 3.0255(4) Å, which is characteristic of an aurophilic interaction (Scheme 5).[59] An intermolecular interaction between the phosphine oxide group of one monomer and the gold cationic center of the other one was observed, featuring a distance of 2.091(1) Å between the Au and O atoms. Thus, this XRD structure confirmed that the pending arm bearing the phosphine oxide group could change its conformation to set the coordination to a cationic gold center.

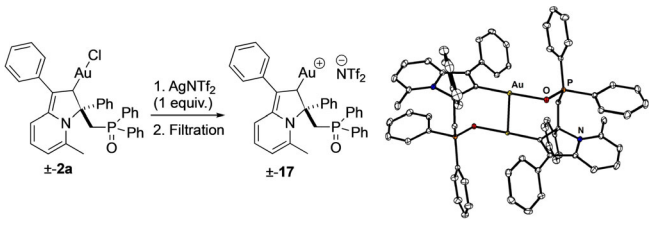

Scheme 5. Synthesis of the cationic catalyst ±-**17** and XRD structure.

DFT calculations were also performed to get insight into the mechanism of the cyclisation of a γ-allenol in order to figure out the crucial role of the phosphine oxide moiety and of the tosylate anion in the cycloisomerization process. Indeed, it appeared that the enantioselective induction was rather effective only in the case where a phosphine oxide was present on the carbene ligand in combination with a tosylate as counterion pointing out a possible participation of these two polar functional groups (see Table 2).

Although an *inner*-sphere mechanism was initially proposed by Telles in 1998 to describe the gold(I)-catalyzed addition of methanol onto alkynes,[60] the *outer*-sphere mechanism for the addition of an O- or N-nucleophile to a gold-coordinated C–C multiple bond complex has received much more experimental and theoretical supports.[54,61] Nevertheless, gold complexes with ligands bearing a judiciously positioned pendant donor function, such as a phosphine oxide[62] or an amine,[63] may favour a *syn*-addition through an *inner*-sphere mechanism. The polar function might also play an active role in the proton transfer steps thanks to its hydrogen-bond acceptor capability.[62] Concerning transformations involving allenes, an *inner*-sphere mechanism supported by calculations has already been put forward for the intramolecular cyclisation of γ-amino allenes when a bis-gold phosphine complex was used.[64]

In the following DFT study, we considered the *inner*- and *outer*-sphere mechanisms for the cycloisomerization of a γ-allenol yielding to a respective *syn*- and *anti*-addition of the hydroxy group onto the gold-activated allene.[65] As mentioned earlier, the presence of the tosylate anion is crucial and therefore its involvement has been taken into consideration. Calculations were performed with the complex (*R*)-**2a·OTs**. Hexa-4,5-dien-1-ol **18** was used as a model to compute the formation of the (*R*)-vinyltetrahydrofuran product (Figure 3a). As non-polar solvents gave the best results in terms of reactivity and enantioselectivity, it can be assumed that the tosylate anion stays rather close to the gold complex during the whole substrate transformation. Thereby, we considered two starting gold-allene η^2 complexes **I** and **I′** with the tosylate anion interacting either with the metal or with the heterocyclic ring, respectively. In the latter complex **I′,** which is slightly less stable than **I** by 1.5 kcal mol^{-1}, the electron-rich oxygen of the phosphine oxide is pointing towards the electrophilic metal (d Au-O = 3.62 Å) and therefore is located in a suitable position to adopt an appropriate conformation for interactions with the coordinated substrate. A transition state for the *inner*-sphere mechanism involving unambiguous hydrogen bonding between the phosphine oxide and the hydroxyl group could be computed (blue pathway, Figure 3a). The optimised structure **(*S*)-TS$_{SYN'}$** displays an activation barrier of 14.0 kcal mol^{-1} as a consequence of a beneficial template effect. The nucleophilicity of the hydroxyl group is enhanced by the proximity of the hydrogen-bond acceptor which also accounts for the lower energy barrier observed. The cyclization is endergonic by 9.8 kcal mol^{-1} from **I′** and lead to the intermediate **(*R*)-II′** where the protonated tetrahydrofuran is intramolecularly stabilised by the phos-

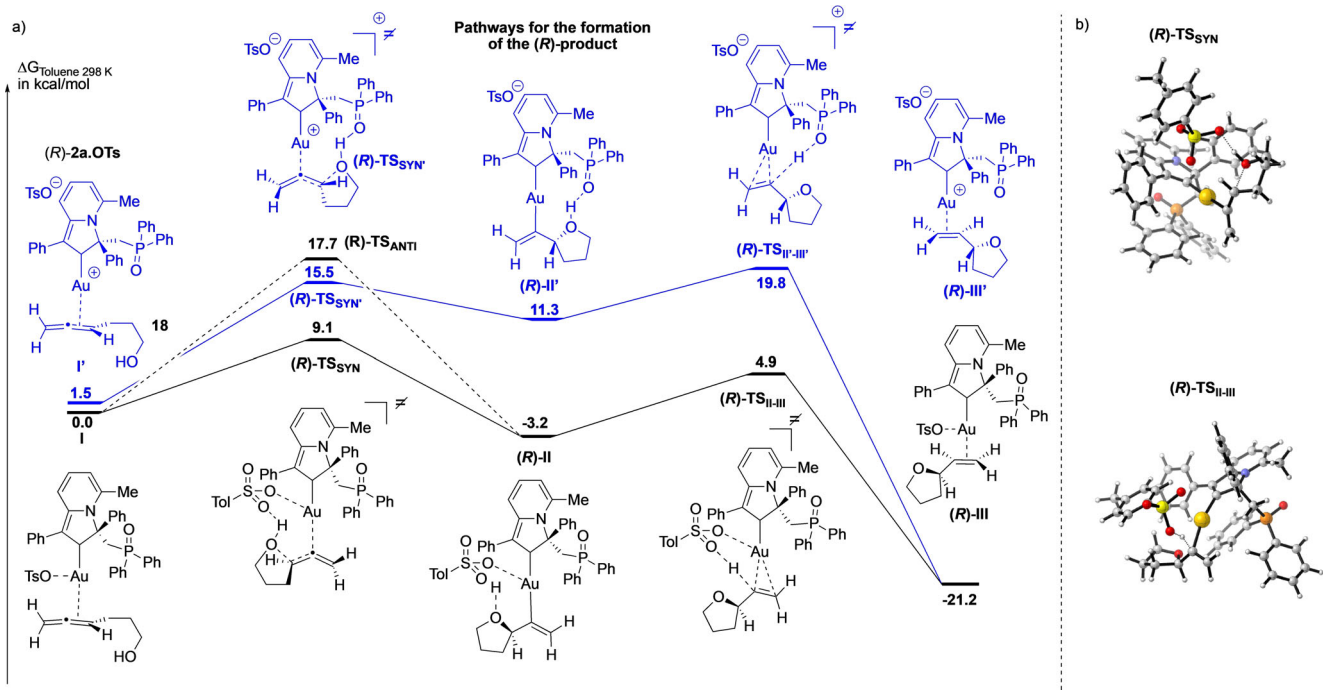

Figure 3. a) Gibbs energy profile for the enantioselective cycloisomerization of γ-allenol **18** in the presence of (*R*)-**2a**·**OTs** at the M06/def2-QZVP(Au)-6–311 + G(2d,p)//B3LYP-D3/SDD(Au)-6-31G(d,p) level of theory (CPCM solvent = toluene). **(*R*)-TS$_{ANTI}$** is obtained from an isoenergetic isomer of **I** with the metal complexed to the other face of the double bond. b) Visualization of the transition states for the cylization and protodeauration steps.

phine oxide. Reversibility in the cyclization of γ-allenols due to ring constraints has already been evidenced experimentally by the groups of Gagné and Widenhoefer.[61c] The next elementary step to form the desired product is the protodeauration. This step usually requires the assistance of an exogenous molecule playing the role of a proton shuttle.[61b,66] Once again, the phosphine oxide group is ideally placed to act this way and operates similarly to a molecular crane by first picking up the proton to deliver it to the reactive C-Au bond. This promotes the protodeauration and furnishes the gold(I)-complexed product **(*R*)-III′**.

The transition state **(*R*)-TS$_{II'\text{-}III'}$** is located 18.3 kcal mol^{-1} above the starting intermediate **I′**. The overall cycloisomerization process is highly exergonic with an associated energy gain of about 20 kcal mol^{-1} that totally drives the reaction despite the first endergonic step. In such a case, the tosylate does not play an active role in the transformation. This pathway is very similar to the one calculated with the cationic complex of (*R*)-**2a** (not taking the anion into consideration, see SI). Even though the stereogenic center is installed during the cyclisation, this internal addition is presumably reversible and the small energy barrier to go backwards (about 4 kcal mol^{-1}) implies a fast equilibrium. Therefore, the final and irreversible protodeauration step would be the actual stereochemically determining event.[67]

However, the tosylate anion is not a weakly coordinating anion and therefore can be involved in the cyclization and the protodeauration steps (black pathway, Figure 3a). Indeed, the activation barrier to reach **(*R*)-TS$_{SYN}$** from the starting intermediate **I** is only 9.1 kcal mol^{-1}. The tosylate, which is coordinated to the gold center, stabilizes the cyclization transition state through hydrogen bonding. The resulting vinylgold intermediate **(*R*)-II** is more stable than **(*R*)-II′** by 14.5 kcal mol^{-1} and the cyclization becomes exergonic. The *anti*-addition without the assistance of the tosylate anion was also computed with a corresponding transition state **(*R*)-TS$_{ANTI}$** lying about 9 kcal mol^{-1} above the *syn*-addition. The protodeauration step can also be assisted by the tosylate. The transient *p*-toluenesulfonic acid delivers the proton to the C-Au bond through **(*R*)-TS$_{II\text{-}III}$** with an activation barrier of only 8.1 kcal mol^{-1} from **(*R*)-II** to lead to the final intermediate **(*R*)-III**. Interestingly, in this pathway with the tosylate coordinated to the gold center, the oxygen of the phosphine oxide prefers to point towards the electron-deficient *N*-containing heterocyclic ring (d O-N = 2.96 Å in structure **I**). The favored interaction brings some rigidity to the system and forces the phosphine oxide moiety to display its two aromatic substituents nearby the chiral active catalytic site, which rationalizes the influence of the aromatic rings substitution on the enantioinduction. In this pathway, the cyclization is the stereochemically-determining step. Gratifyingly, the formation of the (*S*)-vinyltetrahydrofuran product could be computed as well and the transition state corresponding to the cyclization step is higher than the one calculated for the (*R*)-product by 1.3 kcal mol^{-1} (see SI). Although this DFT study has been carried out with a simpler model, the results are consistent with the finding that allenol **13a** is converted into (*R*)-**14a** using (*R*)-**2a** and analogues as precatalysts.

Conclusion

In summary, we have designed a new family of gold(I) complexes based on indolizine-ylidene (Indolizy) ligands. These complexes are readily available from the gold(I)-promoted cyclization of allenylpyridines. The evaluation of the electronic features of the Indolizy ligand has shown highly σ-donor and π-acceptor properties. For that we have relied on a diagnostic reaction and on various NMR analyses. Among others, we used the Huynh's HEP method which had never been used for any carbene other than NHCs. All findings were supported by DFT calculations. Chiral gold(I) complexes could be separated by chiral HPLC and evaluated in asymmetric catalysis. Chiral bifunctional ligands presenting a pending phosphine oxide moiety on the stereogenic center afforded highly efficient and enantioselective cycloisomerizations of γ-functionalized allene derivatives. Increasing the steric demand on the phosphine oxides promoted the best enantiomeric ratios. DFT calculations suggested several possible scenarios highlighting the crucial roles of the phosphine oxide moiety and the tosylate counterion.

Acknowledgements

The authors thank Sorbonne Université (PhD grant to TM), the Franco Thai Scholarship Program administered by CAMPUS FRANCE, IUF and CNRS for financial support. We are also grateful to Lise-Marie Chamoreau (IPCM) for the XRD data and Manon Louis for the studies related to **2h**.

Conflict of Interest

The authors declare no conflict of interest.

Keywords: asymmetric catalysis · carbene · DFT · gold · phosphine oxide

[1] a) *Homogenous Gold Catalysis* (Eds.: V. Michelet, F. D. Toste), Imperial College Press, London, **2014**; b) *Modern Gold Catalysis Synthesis* (Eds.: A. S. K. Hashmi, F. D. Toste), Wiley, Hoboken, **2012**.

[2] For recent reviews, see: a) L. Fensterbank, M. Malacria, *Acc. Chem. Res.* **2014**, *47*, 953 – 965; b) R. Dorel, A. M. Echavarren, *Chem. Rev.* **2015**, *115*, 9028 – 9072; c) D. Pflästerer, A. S. K. Hashmi, *Chem. Soc. Rev.* **2016**, *45*, 1331 – 1367; d) R. Herrera, M. C. Gimeno, *Chem. Rev.* **2021**, https://doi.org/10.1021/acs.chemrev.0c00930; e) C. C. Chintawar, A. K. Yadav, A. Kumar, S. P. Sancheti, N. T. Patil, *Chem. Rev.* **2021**, https://doi.org/10.1021/acs.chemrev.0c00903; f) D. Campeau, D. F. Leon Rayo, A. Mansour, K. Muratov, F. Gagosz, *Chem. Rev.* **2020**, https://doi.org/10.1021/acs.chemrev.0c00788; g) M. Mato, A. Franchina, C. Garcia-Morales, A. M. Echevarren, *Chem. Rev.* **2020**, https://doi.org/10.1021/acs.chemrev.0c00697; h) R. L. Reyes, T. Iwai, M. Sawamura, *Chem. Rev.* **2020**, https://doi.org/10.1021/acs.chemrev.0c00793.

[3] Z. Lu, G. B. Hammond, B. Xu, *Acc. Chem. Res.* **2019**, *52*, 1275 – 1288.

[4] W. Zi, F. D. Toste, *Chem. Soc. Rev.* **2016**, *45*, 4567 – 4589.

[5] a) W. A. Herrmann, *Angew. Chem. Int. Ed.* **2002**, *41*, 1290 – 1309; *Angew. Chem.* **2002**, *114*, 1342 – 1363; b) S. Díez-González, N. Marion, S. P. Nolan, *Chem. Rev.* **2009**, *109*, 3612 – 3676; c) F. Glorius , *N-Heterocyclic Carbenes in Transition Metal Catalysis*, *Vol. 21* (Ed.: F. Glorius), Springer, Berlin/Heidelberg, **2007**; d) M. N. Hopkinson, C. Richter, M. Schedler, F. Glorius, *Nature* **2014**, *510*, 485 – 496.

[6] a) H. Jacobsen, A. Correa, A. Poater, C. Costabile, L. Cavallo, *Coord. Chem. Rev.* **2009**, *253*, 687 – 703; b) D. J. Nelson, S. P. Nolan, *Chem. Soc. Rev.* **2013**, *42*, 6723 – 6753; c) T. Dröge, F. Glorius, *Angew. Chem. Int. Ed.* **2010**, *49*, 6940 – 6952; *Angew. Chem.* **2010**, *122*, 7094 – 7107; d) D. Gatineau, J.-P. Goddard, V. Mansuy, L. Fensterbank, *Isr. J. Chem.* **2013**, *53*, 892 – 900.

[7] a) V. Lavallo, Y. Canac, C. Präsang, B. Donnadieu, G. Bertrand, *Angew. Chem. Int. Ed.* **2005**, *44*, 5705 – 5709; *Angew. Chem.* **2005**, *117*, 5851 – 5855; b) M. Soleilhavoup, G. Bertrand, *Acc. Chem. Res.* **2015**, *48*, 256 – 266.

[8] M. Melaimi, R. Jazzar, M. Soleihavoup, G. Bertrand, *Angew. Chem. Int. Ed.* **2017**, *56*, 10046 – 10068; *Angew. Chem.* **2017**, *129*, 10180 – 10203.

[9] R. Jazzar, M. Soleilhavoup, G. Bertrand, *Chem. Rev.* **2020**, *120*, 4141 – 4168.

[10] a) V. Lavallo, G. D. Frey, B. Donnadieu, M. Soleilhavoup, G. Bertrand, *Angew. Chem. Int. Ed.* **2008**, *47*, 5224 – 5228; *Angew. Chem.* **2008**, *120*, 5302 – 5306; b) R. Kinjo, B. Donnadieu, G. Bertrand, *Angew. Chem. Int. Ed.* **2011**, *50*, 5560 – 5563; *Angew. Chem.* **2011**, *123*, 5674 – 5677.

[11] B. Rao, H. Tang, X. Zeng, L. Liu, M. Melaimi, G. Bertrand, *Angew. Chem. Int. Ed.* **2015**, *54*, 14915 – 14919; *Angew. Chem.* **2015**, *127*, 15128 – 15132.

[12] D. Janssen-Müller, C. Schlepphorst, F. Glorius, *Chem. Soc. Rev.* **2017**, *46*, 4845 – 4854.

[13] For review on complexes of coinage metals with chiral NHCs, see: S. Budagumpi, R. S. Keri, G. Achar, K. N. Brinda, *Adv. Synth. Catal.* **2020**, *362*, 970 – 997.

[14] Y. Matsumoto, K. S. Selim, H. Nakanishi, K.-I. Yamada, Y. Yamamoto, K. Tomioka, *Tetrahedron Lett.* **2010**, *51*, 404 – 406.

[15] D. Banerjee, A. K. Buzas, C. Besnard, E. P. Kündig, *Organometallics* **2012**, *31*, 8348 – 8354.

[16] B. W. Gung, M. R. Holmes, C. A. Jones, R. Ma, C. L. Barnes, *Tetrahedron Lett.* **2016**, *57*, 3912 – 3915.

[17] < For a recent review on chiral NHCs see: M. Michalak, W. Kośnik, *Catalysts* **2019**, *9*, 890.

[18] For seminal work on acyclic chiral carbenes, see: S. Handa, L. M. Slaughter, *Angew. Chem. Int. Ed.* **2012**, *51*, 2912 – 2915; *Angew. Chem.* **2012**, *124*, 2966 – 2969.

[19] M. Alcarazo, S. J. Roseblade, A. R. Cowley, R. Fernández, J. M. Brown, J. M. Lassaletta, *J. Am. Chem. Soc.* **2005**, *127*, 3290 – 3291.

[20] C. Burstein, C. W. Lehmann, F. Glorius, *Tetrahedron* **2005**, *61*, 6207 – 6217.

[21] For robust gold(I) complexes bearing a barbituric heterocycle at the C5 position, see: Y. Tang, I. Benaissa, M. Huynh, L. Vendier, N. Lugan, S. Bastin, P. Belmont, V. César, V. Michelet, *Angew. Chem. Int. Ed.* **2019**, *58*, 7977 – 7981; *Angew. Chem.* **2019**, *131*, 8061 – 8065.

[22] J. Francos, F. Grande-Carmona, H. Faustino, J. Iglesias-Sigüenza, E. Díez, I. Alonso, R. Fernández, J. M. Lassaletta, F. López, J. L. Mascareñas, *J. Am. Chem. Soc.* **2012**, *134*, 14322 – 14325.

[23] J.-Q. Zhang, Y. Liu, X.-W. Wang, L. Zhang, *Organometallics* **2019**, *38*, 3931 – 3938.

[24] D. Pichon, M. Soleilhavoup, J. Morvan, G. P. Junor, T. Vives, C. Crévisy, V. Lavallo, J.-M. Campagne, M. Mauduit, R. Jazzar, G. Bertrand, *Chem. Sci.* **2019**, *10*, 7807 – 7811.

[25] For Ru complexes bearing C1-symmetric cyclic CAAC ligands giving high enantioselectivities in asymmetric olefin metathesis, see: J. Morvan, F. Vermersch, Z. Zhang, L. Falivene, T. Vives, V.

Dorcet, T. Roisnel, C. Crévisy, L. Cavallo, N. Vanthuyne, G. Bertrand, R. Jazzar, M. Mauduit, *J. Am. Chem. Soc.* **2020**, *142*, 19895.
[26] F. Kolundžić, A. Murali, P. Pérez-Gálan, J. O. Bauer, C. Strohmann, K. Kumar, H. Waldmann, *Angew. Chem. Int. Ed.* **2014**, *53*, 8122 – 8126; *Angew. Chem.* **2014**, *126*, 8260 – 8264.
[27] F. Schröder, C. Tugny, E. Salanouve, H. Clavier, L. Giordano, D. Moraleda, Y. Gimbert, V. Mouriès-Mansuy, J.-P. Goddard, L. Fensterbank, *Organometallics* **2014**, *33*, 4051 – 4056.
[28] A. Vanitcha, C. Damelincourt, G. Gontard, N. Vanthuyne, V. Mouriès-Mansuy, L. Fensterbank, *Chem. Commun.* **2016**, *52*, 6785 – 6788.
[29] C. Tugny, N. del Rio, M. Koohgard, N. Vanthuyne, D. Lesage, K. Bijouard, P. Zhang, J. Meijide Suárez, S. Roland, E. Derat, O. Bistri-Aslanoff, M. Sollogoub, L. Fensterbank, V. Mouriès-Mansuy, *ACS Catal.* **2020**, *10*, 5964 – 5972.
[30] For a recent example of bifunctional NHC-AuCl complex, see: O. Seppänen, S. Aikonen, M. Muuronen, C. Alamillo-Ferrer, J. Burès, J. Helaja, *Chem. Commun.* **2020**, *56*, 14697 – 14700.
[31] A. Vanitcha, G. Gontard, N. Vanthuyne, E. Derat, V. Mouriès-Mansuy, L. Fensterbank, *Adv. Synth. Catal.* **2015**, *357*, 2213 – 2218.
[32] For recent similar approaches, see: a) H. K. Wagner, H. Wadepohl, J. Ballmann, *Chem. Sci.* **2021**, *12*, 3693 – 3701; b) S. Arndt, M. M. Hansmann, P. Motloch, M. Rudolph, F. Rominger, A. S. K. Hashmi, *Chem. Eur. J.* **2017**, *23*, 2542 – 2547; c) A. S. K. Hashmi, D. Riedel, M. Rudolph, F. Rominger, T. Oeser, *Chem. Eur. J.* **2012**, *18*, 3827 – 3830.
[33] Deposition Numbers 1055996 (for **2a**), 2064282 (for **2c**), 2064283(for **2d**), 2064284 (for **2e**), and 2064285 (for **2f**) contain the supplementary crystallographic data for this paper. These data are provided free of charge by the joint Cambridge Crystallographic Data Centre and Fachinformationszentrum Karlsruhe Access Structures service www.ccdc.cam.ac.uk/structures.
[34] a) For a review, see: Y. Wang, M. E. Muratore, A. M. Echavarren, *Chem. Eur. J.* **2015**, *21*, 7332 – 7339; b) See also: M. Joost, L. Estevez, S. Mallet-Ladeira, K. Miqueu, A. Amgoune, D. Bourissou, *Angew. Chem. Int. Ed.* **2014**, *53*, 14512 – 14516; *Angew. Chem.* **2014**, *126*, 14740 – 14744.
[35] H. K. Maliszewska, D. L. Hughes, M. P. Muñoz, *Dalton Trans.* **2020**, *49*, 4034 – 4038.
[36] Deposition Number 2081677 (for (−)-(*S*)-**2a**) contains the supplementary crystallographic data for this paper. These data are provided free of charge by the joint Cambridge Crystallographic Data Centre and Fachinformationszentrum Karlsruhe Access Structures service www.ccdc.cam.ac.uk/structures.
[37] See supporting information and also ref. [28].
[38] J. K. E. T. Berton, H. Salemi, J.-L. Pirat, D. Virieux, C. V. Stevens, *J. Org. Chem.* **2017**, *82*, 12439 – 12446.
[39] Deposition Number 2064286 (for **2k**) contains the supplementary crystallographic data for this paper. These data are provided free of charge by the joint Cambridge Crystallographic Data Centre and Fachinformationszentrum Karlsruhe Access Structures service www.ccdc.cam.ac.uk/structures.
[40] H. V. Huynh, *Chem. Rev.* **2018**, *118*, 9457 – 9492.
[41] A. A. Tukov, A. T. Normand, M. S. Nechaev, *Dalton Trans.* **2009**, 7015 – 7028.
[42] H. Song, H. Kim, E. Lee, *Angew. Chem. Int. Ed.* **2018**, *57*, 8603 – 8607; *Angew. Chem.* **2018**, *130*, 8739 – 8743.
[43] a) D. Munz, *Organometallics* **2018**, *37*, 275 – 289; b) D. M. Andrada, N. Holzmann, T. Hamadi, G. Frenking, *Beilstein J. Org. Chem.* **2015**, *11*, 2727 – 2736.
[44] E. A. Carter, W. A. Goddard III, *J. Phys. Chem.* **1986**, *90*, 998 – 1001.
[45] S. Guo, H. Sivaram, D. Yuan, H. V. Huynh, *Organometallics* **2013**, *32*, 3685 – 3696.
[46] Q. Teng, H. V. Huynh, *Dalton Trans.* **2017**, *46*, 614 – 627.
[47] Deposition Number 2064288 (for **6**) contains the supplementary crystallographic data for this paper. These data are provided free of charge by the joint Cambridge Crystallographic Data Centre and Fachinformationszentrum Karlsruhe Access Structures service www.ccdc.cam.ac.uk/structures.
[48] A. Liske, K. Verlinden, H. Buhl, K. Schaper, C. Ganter, *Organometallics* **2013**, *32*, 5269 – 5272.
[49] S. V. C. Vummaleti, D. J. Nelson, A. Poater, A. Gomez-Suarez, D. B. Cordes, A. M. Z. Slawin, S. P. Nolan, L. Cavallo, *Chem. Sci.* **2015**, *6*, 1895 – 1904.
[50] For the reaction of related allenyl pyridines with I_2, see: T. Martinez, I. Alahyen, G. Lemière, V. Mouriès-Mansuy, L. Fensterbank, *Org. Process Res. Dev.* **2020**, *24*, 817 – 821.
[51] Deposition Number 2064288 (for **6**) contains the supplementary crystallographic data for this paper. These data are provided free of charge by the joint Cambridge Crystallographic Data Centre and Fachinformationszentrum Karlsruhe Access Structures service www.ccdc.cam.ac.uk/structures.
[52] a) B. Trillo, F. Lopez, S. Montserrat, G. Ujaque, L. Castedo, A. Lledos, J. L. Mascarenas, *Chem. Eur. J.* **2009**, *15*, 3336 – 3339; b) I. Alonso, B. Trillo, F. Lopez, S. Montserrat, G. Ujaque, L. Castedo, A. Lledos, J. L. Mascarenas, *J. Am. Chem. Soc.* **2009**, *131*, 13020 – 13030; c) P. Mauleón, R. M. Zeldin, A. Z. Gonzalez, F. D. Toste, *J. Am. Chem. Soc.* **2009**, *131*, 6348 – 6348; d) J. Petuškova, H. Bruns, M. Alcarazo, *Angew. Chem. Int. Ed.* **2011**, *50*, 3799 – 3802; *Angew. Chem.* **2011**, *123*, 3883 – 3886; e) A. H. Christian, Z. L. Niemeyer, M. S. Sigman, F. D. Toste, *ACS Catal.* **2017**, *7*, 3973 – 3978.
[53] It should be noted that thiophosphine complex **2h** is not stable in the catalytic reaction conditions.
[54] Z. Zhang, R. A. Widenhoefer, *Angew. Chem. Int. Ed.* **2007**, *46*, 283 – 285; *Angew. Chem.* **2007**, *119*, 287 – 289.
[55] a) Z. Wang, C. Nicolini, C. Hervieu, Y.-F. Wong, G. Zanoni, L. Zhang, *J. Am. Chem. Soc.* **2017**, *139*, 16064 – 16067; b) J. L. Arbour, H. S. Rzepa, J. Contreras-García, L. A. Adrio, E. M. Barreiro, K. K. (Mimi) Hii, *Chem. Eur. J.* **2012**, *18*, 11317 – 11324.
[56] C. Bartomolé, D. Garcia-Cuadrado, Z. Ramiro, P. Espinet, *Inorg. Chem.* **2010**, *49*, 9758 – 9764.
[57] N. Mézailles, L. Ricard, F. Gagosz, *Org. Lett.* **2005**, *7*, 4133 – 4136.
[58] Deposition Number 2064289 (for **17**) contains the supplementary crystallographic data for this paper. These data are provided free of charge by the joint Cambridge Crystallographic Data Centre and Fachinformationszentrum Karlsruhe Access Structures service www.ccdc.cam.ac.uk/structures.
[59] H. Schmidbaur, A. Schier, *Chem. Soc. Rev.* **2008**, *37*, 1931 – 1951.
[60] J. H. Teles, S. Brode, M. Chabanas, *Angew. Chem. Int. Ed.* **1998**, *37*, 1415 – 1418; *Angew. Chem.* **1998**, *110*, 1475 – 1478.
[61] a) R. S. Paton, F. Maseras, *Org. Lett.* **2009**, *11*, 2237 – 2240; b) Z. J. Wang, D. Benitez, E. Tkatchouk, W. A. Goddard III, F. D. Toste, *J. Am. Chem. Soc.* **2010**, *132*, 13064 – 13071; c) T. J. Brown, D. Weber, M. R. Gagné, R. A. Widenhoefer, *J. Am. Chem. Soc.* **2012**, *134*, 9134 – 9137; d) R. J. Harris, R. G. Carden, A. N. Duncan, R. A. Widenhoefer, *ACS Catal.* **2018**, *8*, 8941 – 8952.
[62] C. Hahn, L. Cruz, A. Villalobos, L. Garzaa, S. Adeosun, *Dalton Trans.* **2014**, *43*, 16300 – 16309.
[63] K. D. Hesp, M. Stradiotto, *J. Am. Chem. Soc.* **2010**, *132*, 18026 – 18029.
[64] J. H. Kim, S.-W. Park, S. R. Park, S. Lee, E. J. Kang, *Chem. Asian J.* **2011**, *6*, 1982 – 1986.
[65] a) E. Soriano, I. Fernández, *Chem. Soc. Rev.* **2014**, *43*, 3041 – 3105; b) M. Malacria, L. Fensterbank, V. Gandon, *Top. Curr. Chem.* **2011**, *302*, 157 – 182.
[66] a) C. M. Krauter, A. S. K. Hashmi, M. Pernpointner, *ChemCatChem* **2010**, *2*, 1226 – 1230; b) G. Ciancaleoni, L. Belpassi, D.

Zuccaccia, F. Tarantelli, P. Belanzoni, *ACS Catal.* **2015**, *5*, 803 – 814.

[67] R. E. M. Brooner, T. J. Brown, M. A. Chee, R. A. Widenhoefer, *Organometallics* **2016**, *35*, 2014 – 2021.

Manuscript received: May 6, 2021
Revised manuscript received: June 21, 2021
Accepted manuscript online: July 9, 2021
Version of record online: ■■ ■■, ■■■■

Research Articles

Asymmetric Catalysis

T. Martinez, A. Vanitcha, C. Troufflard, N. Vanthuyne, J. Forté, G. Gontard, G. Lemière,* V. Mouriès-Mansuy,* L. Fensterbank* _____ ■■■■–■■■■

Indolizy Carbene Ligand. Evaluation of Electronic Properties and Applications in Asymmetric Gold(I) Catalysis

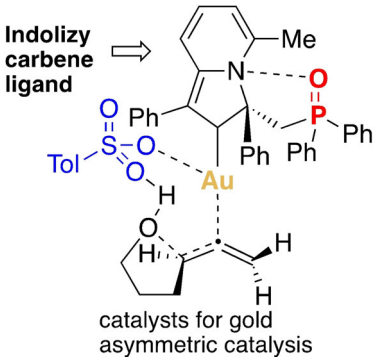

Au^{I} complexes coordinated to the Indolizy ligand, a new carbene ligand that results from the gold-promoted cyclization of a pyridyl-allene were investigated. The electronic properties of the Indolizy ligand were analysed. The introduction of a stereogenic center in α-position to the carbene center coupled to the introduction of a pending phosphine oxide group affords highly efficient and enantioselective Au^{I} catalysts.

These are not the final page numbers!